Electron Ejection from Mo by He^+, He^{++}, and He_2^+

HOMER D. HAGSTRUM
Bell Telephone Laboratories, Murray Hill, New Jersey
(Received September 25, 1952)

Total yield and kinetic energy distribution have been measured for electrons ejected from atomically clean and gas covered molybdenum by the ions He^+, He^{++}, and He_2^+ in the kinetic energy range 10 to 1000 ev. Evidence is presented that one electron is excited into the kinetic energy continuum for each incident He^+ ion and that the electrons so excited are partially internally reflected at the potential barrier of the metal. The slowest ions observed were found to eject 0.25, 0.72, and 0.13 electron per ion for He^+, He^{++}, and He_2^+, respectively. Total electron yield is found to be nearly independent of ion kinetic energy up to 1000 ev. This observation and that of the kinetic energy maximum for slow ions indicate that the electrons are released in an Auger type process for which the energy is supplied by the potential and not the kinetic energy of the ion (potential ejection). Electrons of kinetic energy greater than the upper limit predicted by present theory are observed for faster ions and are accounted for by the shift of the energy levels of the bombarding particle when it is near the metal surface. Some conclusions concerning reflection processes at a metal surface and the nature of electron ejection by the alpha-particle (He^{++}) and the molecular helium ion (He_2^+) come out of this work.

I. INTRODUCTION

EJECTION of an electron from a metal by a positive ion proceeds by the excitation of an electron into the kinetic energy continuum above the surface potential barrier. The energy for this transition may come either from the kinetic or potential energy of the ion. These two possibilities have been distinguished as *kinetic* and *potential ejection*, respectively. Depending upon the kinetic energy range of the ion, kinetic ejection may involve the acceleration by impact inside the metal of free and/or bound electrons some of which escape through the surface,[1,2] or the release of bound electrons from surface atoms.[3,4] The evidence is that kinetic ejection predominates for all ions of kinetic energy greater than a few thousand electron volts and at all speeds in the event potential ejection is energetically impossible.

Potential ejection, on the other hand, involves electronic interaction between the incoming ion and the conduction electrons of the metal while the ion is still outside the metal surface. It can occur when the potential energy recovered on neutralization of the ion is sufficient both to extract the neutralizing electron and to excite a second metal electron to a level above the potential barrier at the surface of the metal. Potential ejection is thus expected to be the predominant mechanism for the case of slow ions of the noble gases incident upon metal surfaces.

Detailed mechanisms of potential ejection have been proposed and investigated theoretically by Oliphant and Moon,[5] Massey,[6] Shekhter,[7] and Cobas and Lamb.[8] Experimental investigations of potential ejection for slow ions of the noble gases include those of Penning,[9,10] Oliphant,[11] Rostagni,[12] and D'Ans, DaRios, and Malaspina.[13] Oliphant[14] and Greene[15] have studied the related ejection of electrons by metastable atoms of the noble gases.

This paper is the report of a study of the secondary electron emission from molybdenum produced by the ions He^+, He^{++}, and He_2^+. The measurements were made with an instrument which provides a focused beam of ions, homogeneous in constitution and energy, whose energy at the target surface can be varied over a wide range. The state of the target surface has been investigated by observation of the rate of adsorption of gas upon it. In this study of potential ejection, it has thus been possible, perhaps for the first time, to meet the rather basic experimental requirement of known ions of known kinetic energy incident upon a target surface demonstrably free from adsorbed atoms. Measurements are reported of total electron yield and of distribution in kinetic energy of the ejected electrons. The dependence of these characteristics on kinetic energy of the incident ion has also been investigated. Discussion of the results in the light of theory is included and comparison with previous experimental results is made.

Notation used in this paper is defined in Table I. Relevant energy constants are listed in Table II.

[1] A. Becker, Ann. Physik **75**, 217 (1924).
[2] G. Schneider, Ann. Physik **11**, 357 (1931).
[3] M. E. Gurtovoy, J. Exptl. Theor. Phys. (U.S.S.R.) **10**, 483 (1940).
[4] W. Ploch, Z. Physik **130**, 174 (1951).
[5] M. L. E. Oliphant and P. B. Moon, Proc. Roy. Soc. (London) **A127**, 388 (1930).
[6] H. S. W. Massey, Proc. Cambridge Phil. Soc. **26**, 386 (1930); **27**, 460 (1931).
[7] S. S. Shekhter, J. Exptl. Theor. Phys. (U.S.S.R.) **7**, 750 (1937).
[8] A. Cobas and W. E. Lamb, Phys. Rev. **65**, 327 (1944).
[9] F. M. Penning, Physica **8**, 13 (1928); Proc. Roy. Acad. Sci. (Amsterdam) **31**, 14 (1928).
[10] F. M. Penning, Proc. Roy. Acad. Sci. (Amsterdam) **33**, 841 (1930).
[11] M. L. E. Oliphant, Proc. Roy. Soc. (London) **A127**, 373 (1930).
[12] A. Rostagni, Z. Physik **88**, 55 (1934); Ricerca sci. **9**, 633 (1938).
[13] D'Ans, DaRios, and Malaspina, Nuovo cimento **5**, 394 (1948).
[14] M. L. E. Oliphant, Proc. Roy. Soc. (London) **A124**, 228 (1929).
[15] D. Greene, Proc. Phys. Soc. (London) **B63**, 876 (1950).

II. THEORETICAL PREDICTIONS CONCERNING POTENTIAL EJECTION

The process of electron ejection by the potential energy recovered when an ion is neutralized at a metal surface is a form of collision of the second kind because in it internal energy is converted to kinetic energy. It is also recognizable as an Auger process in which the excited system metal-ion, on decaying to its ground state, ionizes itself with the ejection of an electron.

Two detailed mechanisms of the electronic transitions involved in potential ejection have been proposed and treated theoretically. One of these is a two-stage process, illustrated in Fig. 1, in which the ion is first neutralized to an excited state by resonance capture of a metal electron, from which state the atom subsequently decays to the ground state with the excitation of a second electron into the kinetic energy continuum. In the case of He^+ incident on Mo, resonance capture occurs to the ^3S metastable level of He, the only excited state isoenergetic to a filled level in the metal (see Fig. 1).

Quantum-mechanical calculations made to date agree in predicting that neutralization by resonance capture (stage 1 of Fig. 2) will occur before the ion can approach the metal surface much closer than several Angstrom units. Shekhter[7] concludes that the probability reaches unity at 3.5A for a 25-ev H^+ ion. Sternberg[16] has recently calculated 4 to 5A as the distance where it becomes highly probable that a 10-ev He^+ ion will be neutralized.

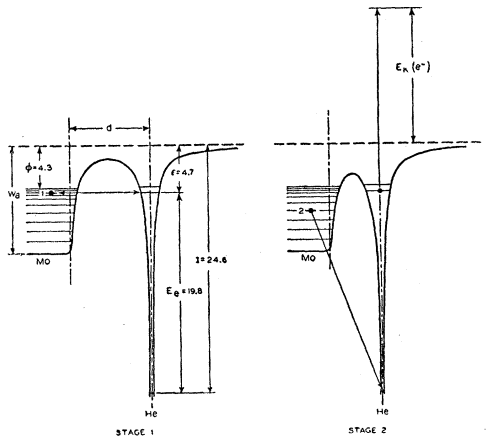

FIG. 1. Electronic transitions characteristic of the so-called two-stage process of potential ejection illustrated for the case of He^+ incident on Mo. Stage 1 consists of the resonance capture by tunneling through the barrier of a conduction electron (1) into the ^3S metastable state of the He atom. In stage 2 the excited atom thus formed is de-excited by capture of second metal electron (2) with the simultaneous excitation of the "metastable" electron into the continuum. State 2 as illustrated here involves electron exchange between metal and atom. Decay of the excited atom without electron exchange (dropping of the "metastable" electron to the ground state and exciting of the second metal electron) is possible but less probable (see text). $E_k(e^-)$ is the kinetic energy the excited electron possesses if it leaves the metal.

[16] D. Sternberg (private communication).

TABLE I. Definitions of notation.

	Particles
e^-	electron
He	normal helium atom
He^M	^3S metastable helium atom
He^+, He^{++}	atomic helium ions
He_2^+	diatomic molecular helium ion
	Energies
I_1	first ionization energy of He ($\rightarrow He^+$)
I_2	second ionization energy of He ($\rightarrow He^{++}$)
I^v	vertical ionization energy of He_2[a]
ϵ	ionization energy of He^M
E_e	electronic excitation energy
E_k	kinetic energy
ϕ	work function
W_i	width of conduction band
W_a	$W_i+\phi$
	Voltages and Currents
V_{ST}	voltage between electrodes S and T (positive when T positive re: S)
V_r	retarding potential, V_{ST}, corrected for contact potential
I_S, I_T	positive currents to electrodes S and T, respectively
	Particle Currents[b]
I^i	primary ionic current entering electrode S
I_i^e	secondary electron current ejected by I^i at T
I_i^i	secondary ionic current from partial reflection of I^i at T
I_i^m	secondary current of metastable atoms from partial reflection of I^i as metastable atoms at T
I_{ie}^e	tertiary electron current ejected from S by I_i^e
I_{ii}^e	tertiary electron current ejected from S by I_i^i
I_{im}^e	tertiary electron current ejected from S by I_i^m
I_r	$I_i^i+I_{ii}^e+I_{im}^e$
	Ejection Coefficients
γ_i, γ_i'	number of electrons ejected per incident ion at T and S, respectively
γ_m, γ_m'	number of electrons ejected per incident metastable atom at T and S, respectively
δ, δ'	number of electrons ejected per incident electron at T and S, respectively
	Reflection Coefficients[c]
R_{ii}	fraction of I^i reflected as ions at T
R_{im}	fraction of I^i reflected as metastable atoms at T
R	$R_{ii}+\gamma_i'R_{ii}+\gamma_m'R_{im}$
	Other Special Symbols
f_k	fraction of electrons comprising I_i^e having kinetic energies $>E_k$
ρ	$I_S/(I_T+I_S)$
z	number of electronic charges carried by primary ion
$z\rho$	$-\gamma_i$ for V_r sufficiently negative
Δp	rise in pressure on target flash
Δt_c	target cold interval
d	distance of ion or atom from metal surface
P	probability that an electron excited into the kinetic energy continuum escapes from the metal.

[a] This quantity is defined and evaluated in reference c of Table II.
[b] The particle currents here defined may or may not involve transport of electric charge. When they do, the symbol also stands for the absolute magnitude of the electric current (see Fig. 4).
[c] These definitions apply only to the case of singly charged ions incident on the target surface.

According to Cobas and Lamb's calculation[8] the decay of He^M by the electron exchange and excitation process (stage 2 of Fig. 1) should proceed with unity probability much nearer the metal surface. Shekhter[7] showed the decay of an excited atom at the metal

TABLE II. Energy constants.

$I_1(\mathrm{He})=24.58$ ev[a]	$\epsilon=I(\mathrm{He}^M)=4.77$ ev[d]
$I_2(\mathrm{He})=78.98$ ev[b]	$\phi(\mathrm{Mo})=4.27$ ev[e]
$I^v(\mathrm{He}_2)\cong 16.8$ ev[c]	$W_i(\mathrm{Mo})\cong 6.5$ ev[f]
$E_e(\mathrm{He}^M)=19.81$ ev[a]	$W_a(\mathrm{Mo})\cong 10.8$ ev

[a] C. E. Moore, *Atomic Energy Levels*, Vol. I, National Bureau of Standards Circular 467 (1949).
[b] $I_2(\mathrm{He})=I_1(\mathrm{He})+I_1(\mathrm{He}^+)=24.58+54.403=78.98$ from reference a.
[c] This is the energy liberated in the transition following electron capture from the stable He_2^+ state to the repulsive He_2 state at constant nuclear separation. The value is that quoted by R. Meyerott, Phys. Rev. **70**, 671 (1946), based on observations by O. S. Duffendack and H. L. Smith, Phys. Rev. **34**, 68 (1929) of spectral enhancement in the $A^2\Pi\rightarrow X^2\Sigma$ system of CO^+ by the molecular ion He_2^+.
[d] $\epsilon=I_1(\mathrm{He})-E_e(\mathrm{He}^M)=24.58-19.81=4.77$ ev.
[e] H. B. Michaelson, J. Appl. Phys. **21**, 536 (1950).
[f] This value is taken to be approximately the same as $W_i(\mathrm{W})$ since W and Mo have the same number of valence electrons and essentially the same lattice constant. M. F. Manning and M. I. Chodorow, Phys. Rev. **56**, 787 (1939) obtained $W_i(\mathrm{W})=0.47R=6.4$ ev from their calculated state density for the six lowest bands of tungsten. This value is in good agreement with the experimental values for the width of the valence band in W of 7.0 ± 0.5 and 6.5 ± 0.5 ev determined by J. A. Bearden and T. M. Snyder, Phys. Rev. **59**, 162 (1941) from transitions from the *5d*, *5s* band to L_{II} and L_{III}, respectively.

surface without electron exchange (the alternative to stage 2 of Fig. 1; see figure caption) to be much less probable, calculating 0.05 for the probability of the process occurring during transit of the ion to and away from the metal.[17]

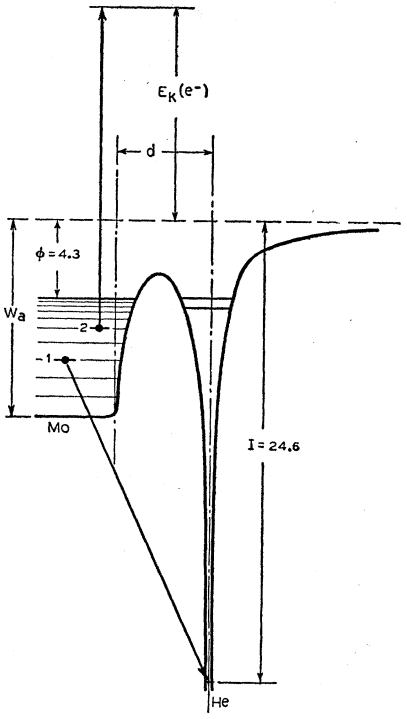

FIG. 2. Electronic transitions involved in the so-called direct process of potential ejection illustrated for He^+ on Mo. The ion is neutralized directly to the ground state with the simultaneous excitation of a second metal electron into the continuum. The metastable levels play no role.

[17] Because of rather drastic simplifying assumptions, calculations of total probabilities, or of the position at which a process proceeds with high probability, should perhaps be trusted only as to relative order of magnitude. Cobas and Lamb, as well as Massey in an earlier calculation (reference 6), used wave functions for the metal electrons which are taken to be zero outside the metal surface. Thus perhaps the most important part of the interaction is neglected. Shekhter used functions which extend outside the metal but found it necessary to simplify the calculations in other ways. Cobas and Lamb have pointed out an error in the matrix element used by Massey.

Theory of the two-stage electron ejection process by He^+ ions on Mo thus indicates that one electron should be excited into the continuum for each ion which strikes the metal surface and that electrons appearing outside the metal should have kinetic energies within the limits specified in Table III.

Shekhter has proposed the so-called direct process of potential ejection illustrated in Fig. 2. His calculation of the total probability of this process gave 0.1. Thus it is much less probable than the two-stage process which presumably predominates when neutralization by resonance capture can occur ($\phi<\epsilon<W_a$). The direct process is of considerable interest for ion-metal combinations for which $\epsilon<\phi$ where it is the only potential ejection process possible. The kinetic energy limits predicted by the direct process for He^+ incident on Mo are included in Table III and indicated on Fig. 13 even though the process is most likely not the predominant one in this case.

Oliphant and Moon[5] discussed neutralization of an ion on the basis of field emission induced by the ion and made the original proposal of the tunneling mechanism of resonance capture as an alternative. Shekhter[7] showed that neutralization of an ion to the ground state accompanied by radiation is very improbable ($\sim 5\times10^{-7}$). There have been no theoretical considerations of potential ejection mechanisms for He^{++} or He_2^+.

TABLE III. Kinetic energy limits of ejected electrons according to mechanisms of Figs. 1 and 2 evaluated for He^+ on Mo.

	Two-stage process (Fig. 1)	Direct process (Fig. 2)
$E_k(e^-)_{\min}$	$I-\epsilon-W_a=9.0$ ev	$I-2W_a=3.0$ ev
$E_k(e^-)_{\max}$	$I-\epsilon-\phi=15.5$ ev	$I-2\phi=16.0$ ev

III. EXPERIMENTAL APPARATUS AND PROCEDURE[18]

The apparatus with which the present experiment was conducted is depicted in Fig. 3. The instrument produces an ion beam, homogeneous in constitution, of total energy spread less than one electron volt. The kinetic energy of the beam at the target surface may be varied conveniently from 10 to 1000 ev. Beam currents are of the order of 5×10^{-10} amp of He^+, 2×10^{-11} amp of He^{++}, and 1×10^{-12} amp of He_2^+ over most of the kinetic energy range.[19]

It is essential to the success of the experiment that no ions strike the edges of the apertures in electrodes M_1, M_2, N, and S and that all ions strike only the target T inside the sphere. For this reason great care

[18] A more detailed account of the experimental apparatus and procedure than that given here is in preparation for submission to *The Review of Scientific Instruments*.

[19] The He_2^+ ions were produced in the ion source at high pressures by the secondary process investigated by J. A. Hornbeck and J. P. Molnar, Phys. Rev. **84**, 621 (1951).

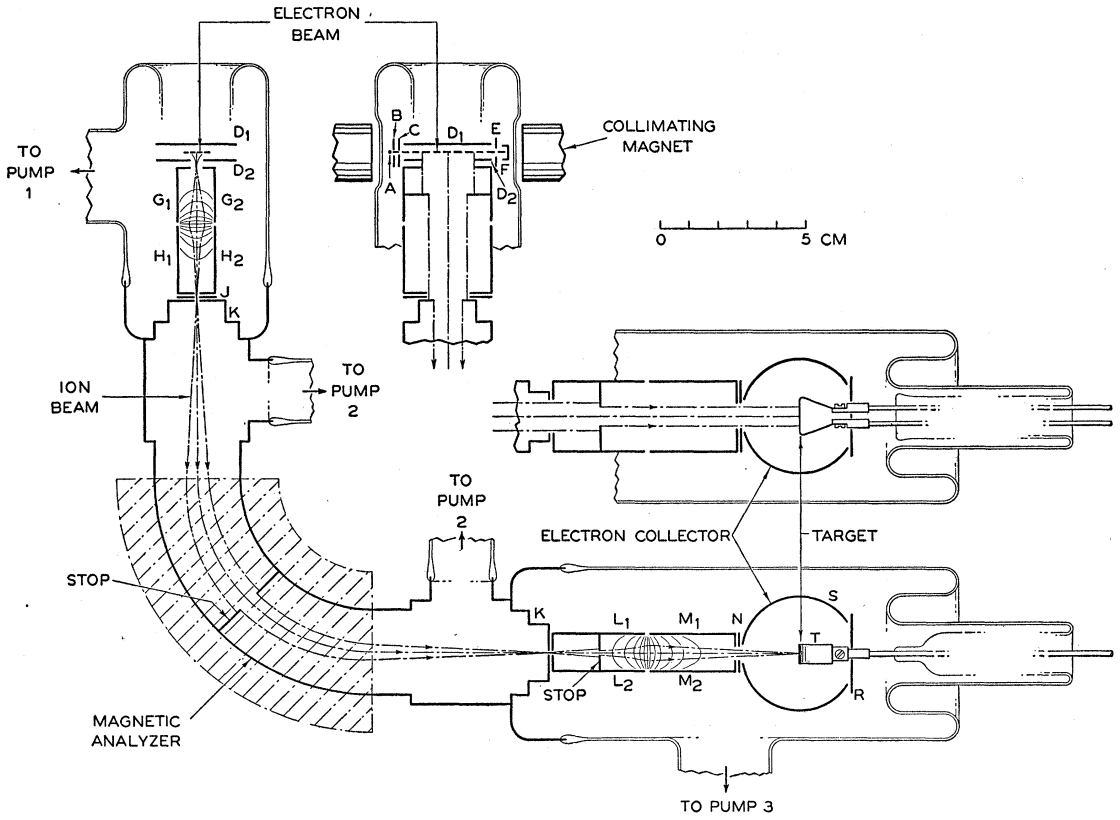

FIG. 3. Schematic diagram of experimental apparatus. The instrument is composed of an electron impact ion source (electrodes A to F), electrostatic ions lenses (G–H and L–M), a magnetic analyzer (K), the target (T), and the spherical electron collector (S). Equipotential lines are indicated in the G–H and L–M lenses. Views of ion source and target-collector ends at 90° from principal view are also shown.

was taken in the design of the $L-M$ lens and the stop between electrodes L_1 and L_2 to see that these conditions were met. Measurements in an auxiliary test apparatus[20] showed the focus to be such that 99.9 percent of the beam strikes within an area 0.2×0.8 cm at the target surface. Since the flat face of the target in the present instrument has the dimensions 0.7×1.4 cm, it is clear that the fraction of the ion beam which misses the target is entirely negligible. That the ion beam is considerably narrower than the target is further demonstrated by the constancy of the currents to S and T (with the current to electrode R equal to zero) for considerable sideways deflection of the beam in either direction by a cross voltage between electrodes M_1 and M_2. This cross voltage was always adjusted so that the beam passed through the center of the entrance aperture in S to strike the center of the target.

The target used in the present experiment was a Mo ribbon 0.0015 in. thick, formed as shown in Fig. 3. It could be heated to 1750°K in a time of the order of one second. Thus desorption of adsorbed gas directly from the target could be accomplished rapidly enough to make adsorption rate studies possible. The size of the target relative to the sphere was made as small as possible, consistent with the requirement that all ions strike it, so that the target-collector geometry would be suitable for determination of electron energy distribution functions by retardation between T and S.

The apparatus is evacuated by three independent two-stage mercury diffusion pumps through traps cooled by liquid nitrogen. Vacuum processing consisted of long periods of pumping with filaments and target hot, heating of the ionization manometer electrodes to red heat by bombardment, and torching of auxiliary glass parts. This was followed by extended pumping with the target cold except for the flashes of short time duration needed to clean it and to make the adsorption rate measurements. After starting the pumps several weeks of processing were needed before data taking commenced. Background pressures were then less than 4×10^{-9} mm Hg as measured with an ionization manometer of the type described by Bayard and Alpert.[21]

[20] Specifications on focus and energy homogeneity of the ion beam quoted here were determined with an apparatus like that of Fig. 3 except that the sphere and target are replaced by a slit system and plane parallel retardation chamber placed at the target position. This apparatus is to be reported on elsewhere (reference 18). It is in fact that used in the study of dissociative ionization by electron impact shown in Fig. 3 of H. D. Hagstrum, Revs. Modern Phys. **23**, 185 (1951).

[21] R. T. Bayard and D. Alpert, Rev. Sci. Instr. **21**, 571 (1950).

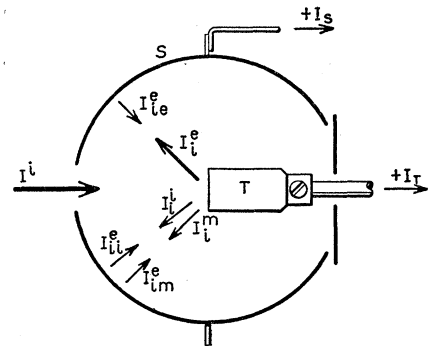

FIG. 4. Schematic diagram of target, T, and electron collector, S, showing primary, secondary, and tertiary particle currents which need to be considered in interpreting retarding potential measurements. The letters e, i, and m in sub- and super-scripts stand for electron, ion, and metastable atom, respectively. The superscript indicates the nature of the particle. For a secondary current the single subscript indicates the primary particle; for a tertiary current the subscripts indicate the primary and secondary particles, respectively. See explicit definitions of each symbol given in Table I.

Always the measured rate of adsorption of gas on the target was taken as the final test of the vacuum and target surface conditions.

Contact potential between target and electron collector was determined by retardation of the thermionic electron current emitted directly from the heated target. In making these measurements, the heating current was pulsed, and measurements made of thermionic current passed between the heating pulses in the manner described by Germer.[22] The primary, secondary, and tertiary currents which flow between S and T are depicted schematically in Fig. 4; the symbolic designations are defined in Table I.

IV. STATE OF THE TARGET SURFACE

For a surface sensitive phenomenon like potential ejection it is essential that one know the state of the target surface. This is emphasized by the observation that a monolayer of nitrogen forms on a tungsten surface in $\frac{2}{3}$ second at 10^{-6} mm Hg pressure.[23] It is clear that specification of evacuation procedure and target processing alone is not sufficient to demonstrate an atomically clean surface. Means for such demonstration is afforded, however, by the measurement of the rate of adsorption of gas upon the target surface.[24] The measurement consists in observing the rise in pressure, Δp, accompanying sudden heating of the metal as a function of previous cold interval, Δt_c, during which the adsorption took place. The flashing of the target at the end of one cold interval and the beginning of another consisted of a 30-second flash followed by two 5-second flashes with one and two minutes cold interval between the first and second and the second and third of these flashes, respectively. This procedure was found to prevent the readsorption of desorbed gas by the target before such gas could be pumped out of the system. Δp was read on the first flash and the instant of cooling after the third flash marked the beginning of the next cold interval. Occasionally, the target was heated for longer periods, particularly after prolonged exposure to the residual gases, to remove absorbed gas and to degas the target supporting leads.

The result of adsorption rate measurements made with the instrument set up for γ_i measurements (He gas being admitted; ion source filament on) is shown in the lower graph of Fig. 5. The Δp *vs* Δt_c curve is seen to pass through a maximum just short of two hours after which the curve levels off to an adsorption rate (slope of the $\Delta p - \Delta t_c$ curve) much smaller than the initial rate. This result is interpreted as indicating the formation in 1.5 to 2 hours of a monoloayer by adsorption from the adsorbable gas component present in the instrument.[23] Simultaneous measurement of γ_i, plotted at the top of Fig. 5 shows a reduction of γ_i for 200-ev He^+ ions as gas covers the surface. The effect saturates when the surface is completely covered as indicated by the adsorption rate measurements. In obtaining these data, the Mo target was flashed to 1500°K.

The data of Fig. 5 were taken with He in the apparatus and the ion source filament on. The pressure of He in the target chamber (about 1/100 of that in the ion source chamber) was about 1×10^{-7} mm Hg. The adsorption rate therefore is determined by the amount of adsorbable impurity introduced with the He as well as the adsorbable component in the residual gas which is slowly desorbed from the internal parts and walls of the instrument itself. An adsorption rate about 20 percent less (monolayer adsorption time about 20 percent greater) was measured with no He being admitted and the ion source filament unheated. An order of magnitude calculation shows that this observation can be accounted for by the introduction with the helium of about 0.3 percent impurity, a not unreasonable amount.

The maximum in the $\Delta p - \Delta t_c$ curve was observed in all measurements in this work when the monolayer adsorption time was greater than about half an hour. This experimental result indicates that if the layer is left on the surface a longer time its later removal results

[22] L. H. Germer, Phys. Rev. **25**, 795 (1925).

[23] The term "monolayer" is used in this paper to denote the surface coverage at which the adsorption rate is observed to decrease from a relatively high constant value to a relatively low value. The time required to reach this condition from an atomically clean condition is termed the "monolayer adsorption time." The example quoted here is based on data of J. A. Becker and C. D. Hartman (private communication; paper submitted to J. Phys. Chem.). The monolayer adsorption time is determined by the kinetic theory rate at which molecules strike the surface, the observed initial sticking probability of 0.5, and the result that the sticking probability begins to fall from this initial constant value when the surface concentration of N atoms reaches 2.5×10^{14} per cm^2.

[24] L. Apker, Ind. Eng. Chem. **40**, 846 (1948). The method was brought to the author's attention in a public discussion of it by W. B. Nottingham in 1948. The author is indebted to his colleagures J. P. Molnar, J. A. Becker, and C. D. Hartman for helpful discussions concerning the adsorption rate measurements.

in a smaller number of gas atoms reaching the ionization gauge. Under these circumstances the remainder of the layer may possibly come off in a form more readily adsorbed or otherwise removed from the gas phase during the many collisions with the walls of the apparatus before reaching the ionization gauge. The effect may perhaps be the result of relatively slow surface migration and chemical rearrangement in the surface layer of more than one adsorbed molecular species. Or it may indicate the slow interaction of the surface layer with a second molecular species arriving at the surface from the surrounding gas. At these low pressures it is difficult to specify the nature of the adsorbable gas component. Earlier in the evacuation procedure, however, the residual gases present in the apparatus, as determined by m/e analysis, were found mainly at $m/e=28$ and 18 (presumably CO and H_2O) in about equal proportions. No ion current was detectable at $m/e=32$ (O_2).

The question remains whether the procedure adopted results in fact in an atomically clean Mo surface. Evidence already presented shows that a flash to 1500°K certainly removes adsorbed gas. To remove more tenaciously held atoms, if any were present, the target was heated to 1750°K for short intervals (minutes) periodically throughout the experiment. This treatment is held adequate to assure an atomically clean Mo surface on the following grounds: it is assumed that flashing to a temperature high enough to remove adsorbed oxygen cleans the metal of any contaminant likely to be present. Unfortunately there are no direct determinations of the temperature needed to remove oxygen from Mo. It is possible, however, to obtain a good estimate from the similar data for W and the observations of the relative temperatures of Mo and W at which several other surface phenomena take place. Langmuir's conclusion is that heating to 2200°K removes oxygen from W.[25] Measurements of degassing rate,[26] nitrogen desorption,[27] thorium evaporation,[28] and mobility of surface atoms[29] all show rates for Mo comparable to those for W when the Mo temperature is about 0.8 that of W. Finally, the work of Gulbransen and Wysong[30] on the evaporation of molybdenum oxides shows that the oxides can be removed readily by heating and that one need not fear a situation for molybdenum like that obtaining for aluminum whose oxides have a lower vapor pressure than the metal itself. For these reasons it was thought safe to conclude that oxygen will be removed from Mo at about 0.8 $\times$2200°K$\cong$1750°K and that this temperature is sufficiently high to remove any other impurity atom from the Mo surface in this experiment. The value of γ_i measured immediately after a target flash (Fig. 5) is thus taken to be characteristic of the atomically clean metal.

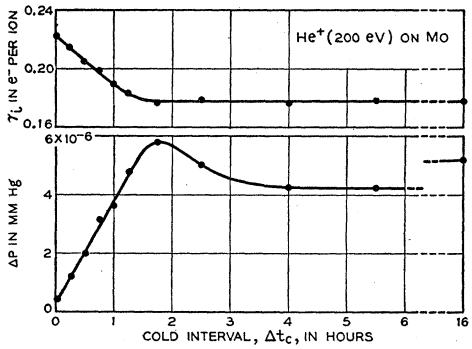

FIG. 5. Plots of γ_i (top) and Δp observed at flash (bottom) for the Mo target as a function of cold interval, Δt_c. He^+ ions of 200-ev kinetic energy were used in obtaining the γ_i data. The target was flashed to 1500°K. Both curves give evidence of a monolayer adsorption time of 1.5 to 2.0 hours. The γ_i value measured within a minute after flash is characteristic of atomically clean Mo, that observed after 2 hours characteristic of Mo with a monolayer of gas adsorbed upon it.

No polishing of the target ribbon was undertaken. The surface on inspection after removal appeared to be thermally etched, clean, and polycrystalline in nature.

V. ELECTRON YIELD (γ_i) AND ITS DEPENDENCE ON THE KINETIC ENERGY

The measurement of total electron yield, γ_i, is made with $V_{ST}=-5$ v. This assures collection of all ejected electrons since electrons are then accelerated to the electron collector. The results are plotted as functions of ion kinetic energy in Fig. 6. Measurements are reproducible to within 5 percent and it is believed that no systematic error of greater than this amount is present in the data.

There are several important features of the results of Fig. 6 to be discussed. First, the fact that γ_i is essentially independent of ion kinetic energy in the range 10 to 1000 ev is to be noted. This is a strong indication of the essential correctness of the potential ejection mechanism for ejection by each of the ions He^+, He^{++}, and He_2^+. The data lead one to expect that very slow ions,

[25] O_2 was found to affect thermionic emission from W at $T<2200$°K [I. Langmuir, J. Am. Chem. Soc. **35**, 105 (1913)]. An oxygen film was removed at 2070°K at a rate such that half disappeared in 20 seconds [I. Langmuir and D. S. Villars, J. Am. Chem. Soc. **53**, 495 (1931)]. See also I. Langmuir, *Phenomena, Atoms and Molecules* (Philosophical Library, New York, 1950), p. 35 ff.

[26] F. J. Norton and A. L. Marshall, Trans. Am. Inst. Mining Met. Engrs. **156**, 351 (1944), report that with similar previous treatment the degassing rate of Mo at 2100°K is comparable to that of W near 2650°K.

[27] J. A. Becker and C. D. Hartman, private communication, observe that adsorbed nitrogen is completely removed at and above 1500°K from Mo, above 1800°K from W.

[28] M. Benjamin and R. O. Jenkins, Proc. Roy. Soc. (London) **A180**, 225 (1942), report that thorium starts to evaporate from Mo at 1700°K, from W at 2100°K. See also R. O. Jenkins, Rep. Prog. Phys. **9**, 177 (1942–43).

[29] From observations with the field emission microscope Benjamin and Jenkins (reference 28) find Mo atoms becoming mobile on Mo at 770°K, W on W at 1170°K. E. W. Müller, Z. Physik **108**, 668 (1938) quotes 1100°K for this latter temperature.

[30] E. A. Gulbransen and W. S. Wysong, Trans. Am. Inst. Mining Met. Engrs. **175**, 628 (1948).

of thermal velocities perhaps, would eject electrons with efficiencies comparable to those measured in this experiment. In this respect the present data agree with the results of previous workers. However, the results of Oliphant,[11] Rostagni,[12] and D'Ans, DaRios and Malaspina,[13] indicating a rise of $\gamma_i(He^+)$ to near unity or above in the vicinity of 1000-ev kinetic energy are not supported by the present results. The present results are more in agreement with the results of Penning[10] concerning the dependence of γ_i on ion kinetic energy for noble gas ions. The value of 0.17 for $\gamma_i(He^+)$ on Mo at low velocities obtained in previous studies[11–13] agrees well with the value obtained here (Fig. 6) for gas covered molybdenum. This is most likely an indication that the surfaces used in the earlier work were contaminated as the experimental procedure used would also lead one to expect.

A second feature of the data of Fig. 6 is the dependence of γ_i on the nature of the incident ion. Taking the data at low ion energies as representative of pure potential ejection it is seen that $\gamma_i(He^{++}):\gamma_i(He^+):\gamma_i(He_2^+)=0.72:0.25:0.13=2.9:1:0.52$. It is of interest to compare these ratios to the relative magnitudes of potential energy made available by the ion after its neutralization. Using the data of Table II one finds:

$$[I_2(He)-2\phi]:[I_1(He)-\phi]:[I^v(He_2)-\phi]$$
$$=[79.0-2\times4.3]:[24.6-4.3]:[16.8-4.3]$$
$$=3.5:1:0.62.$$

This sequence of γ_i magnitudes, together with the observation that the average electron ejected by He^{++} is not much more energetic than that ejected by He^+ (Sec. VI), suggests that an ion ejects electrons at a metal surface by potential ejection approximately in proportion to the potential energy it can make available at the metal surface on neutralization. This would follow in the case of the doubly charged ion if the decay to the ground state were to proceed through a series of excited states of the singly charged ion and the neutral atom, one electron being excited into the continuum at each step. Sternberg[16] has pointed out that the spread of the wave function of an electron in a high lying excited state will make neutralization to such a state more probable than to a lower state thus favoring the "cascade" type of ejection mechanism for multiply charged ions.

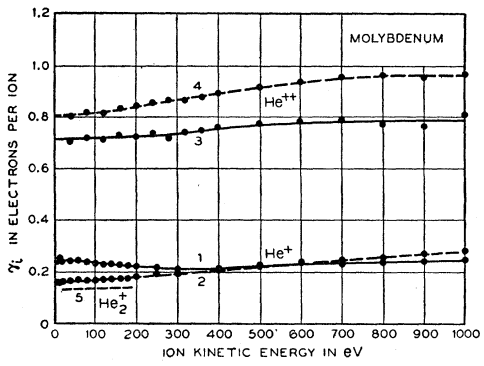

FIG. 6. Plot of experimental data giving total electron yield, γ_i, as a function of ion kinetic energy for the ions He^+ (curves 1 and 2), He^{++} (curves 3 and 4), and He_2^+ (curve 5) on Mo. Curves 1 and 3 are for atomically clean Mo, curves 2, 4, and 5 for Mo covered with a monolayer of gas. Data for He_2^+ lie within 30 percent of line 5.

There remains the possibility, however, that ejection by He^{++} consists of excitation of a single electron which then divides its energy among several other electrons as occurs in secondary emission by incident electrons. Under these circumstances one would expect $\gamma_i(He^{++})=\delta(70.4$ ev) since the electron formed by absorption of all the potential energy of He^{++} is the equivalent of a 70.4-ev electron entering from outside the metal surface. Bruining[31] has published data of Copeland on δ for Mo which show $\delta(70.4$ ev$)\cong0.7$. Thus, as far as magnitude is concerned, $\gamma_i(He^{++})$ could be explained in this way. However, in view of the results for He^+, one should perhaps expect at least a measurable proportion of the electrons excited inside the metal with maximum kinetic energy to be observed outside the metal. The fact that no electrons of energies greater than about 40 ev are observed from He^{++} in this work (Fig. 11) militates against this mechanism of potential ejection by multiply charged ions.

A third point of interest is the magnitude of $\gamma_i(He^+)=0.25$ for slow ions and what it means in view of the theoretical conclusion that one electron is excited into the kinetic energy continuum for each incident He^+ ion. First it should be pointed out that this conclusion is supported by the observation that the quantity R is small, indicating that few ions incident normally to the surface are reflected as ions or metastable atoms. Since radiative neutralization has also been shown to be small,[7] it is difficult to escape the conclusion that one electron is in fact excited into the kinetic energy continuum by each incident ion. The value of γ_i which results depends then solely on the probability, P, that the excited electrons will escape from the metal. We shall assume throughout this discussion that the velocity vectors of the excited electrons are randomly directed.

If the excited electrons start from a point outside the metal surface, as the representation of stage 2 in Fig. 1 suggests, the probability of escape, P, should be at least 0.5 since the electrons which enter the metal may be partially reflected or may excite other electrons which escape. If the electrons were freed inside the potential barrier at the metal surface the possibility of internal reflection at the barrier would reduce P below 0.5.

It can be shown that an electron of total kinetic energy E_k inside the metal incident on a barrier of

[31] H. Bruining, *Die Sekundär-Elektronen-Emission fester Körper* (Springer-Verlag, Berlin, 1942), Fig. 30, p. 22. The author is indebted to his colleague K. G. McKay for a helpful discussion of this point.

height W_a will be internally reflected if its velocity vector makes an angle, θ, with the surface normal greater than $\theta_c=\cos^{-1}(W_a/E_k)^{\frac{1}{2}}$ (see Fig. 7). An electron incident at $\theta<\theta_c$ can escape. The probability of escape can be determined by integration over the solid angle included in the cone of semi-angle θ_c about the surface normal. Thus

$$P=(1/4\pi)\int_0^{\theta_c} 2\pi \sin\theta d\theta=\tfrac{1}{2}(1-\cos\theta_c)=\tfrac{1}{2}[1-(W_a/E_k)^{\frac{1}{2}}].$$

For the two stage process of Fig. 1 electrons could be excited inside the metal to total kinetic energies, E_k, in the range $I-\epsilon$ to $I-\epsilon+W_i$. Using the constants characteristic of He^+ and Mo, the probability P ranges from 0.13 to 0.18. γ_i, which represents an average of P over all possible excited electrons, would lie somewhere within this range if all electrons start inside the metal. The experimental observation of $\gamma_i=0.25$ then suggests that the excited electrons start from a point only part way inside the potential barrier of the metal. This conclusion is compatible with the process of Fig. 1 if the second stage occurs when the atom has penetrated into the potential barrier.

The mechanism proposed above which reduces γ_i below the value 0.5 is internal reflection of electrons incident on the barrier at greater than a critical angle to the surface normal. The quantum-mechanical reflection of electrons incident normally to the barrier and having kinetic energy greater than the barrier height is negligible for the 20-ev electrons encountered here.[32] The above picture of release of the ejected electron inside the metal barrier is not to be confused with the suggestion of Oliphant and Moon[5] that ions may be neutralized inside the metal surface nor with Massey's conjectures[6] (later disputed by Cobas and Lamb[8]) concerning emission of electrons in a cone at the metal surface. Shekhter's objection[7] to the unity transition probability calculated for the potential ejection process of Fig. 1 on the grounds that the measured γ_i is much less than unity appears not to be valid.

The transit time for an ion through the experimental apparatus from ion source to target is about 0.5 microsecond. Any excited ion would certainly decay to its ground state by radiation early in its transit through the instrument. Thus no effect on γ_i of excited ions or radiation from such ions is expected.

The potential ejection by He_2^+ is conceived to proceed by neutralization of He_2^+ resulting in dissociation to two normal He atoms. The energy by which the ground state of He_2^+ lies above the repulsive potential curves of He_2 at the same nuclear separation is recovered and used to extract the neutralizing electron and to excite a second electron (see reference c of Table II).

[32] L. A. MacColl, Bell System Tech. J. **30**, 888 (1951), Fig. 4. See discussion in C. Herring and M. H. Nichols, Revs. Modern Phys. **21**, 185 (1949), Sec. IV. 4.

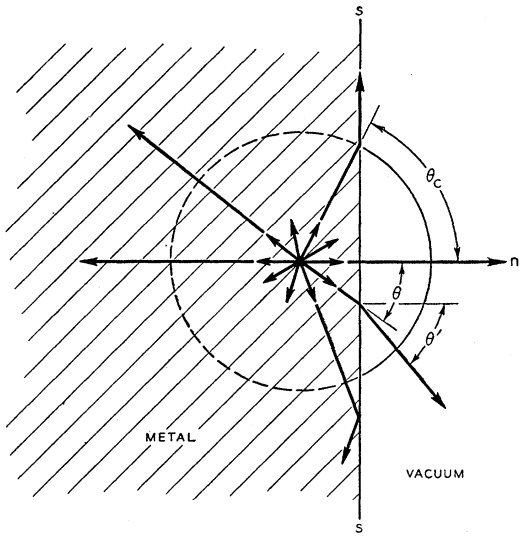

FIG. 7. Schematic diagram of refraction and internal reflection at a metal surface (S–S) of electrons excited into the kinetic energy continuum inside the metal surface barrier with velocity vectors randomly directed. The figure holds for any plane containing a normal (n) to the surface. θ_c is the critical angle for total reflection inside the metal. An electron directed at an angle θ to the surface normal will escape at an angle $\theta'>\theta$ if $\theta<\theta_c$.

VI. ELECTRON ENERGY DISTRIBUTIONS

The kinetic energy distributions of ejected electrons have been determined in this work by applying retarding potentials between target and electron collector. Retarding potential curves for electrons ejected by He^+ ions of 40-, 200-, and 1000-ev energy are plotted in the top graphs of Figs. 8, 9, and 10, respectively. In the lower graphs of these figures are plotted the slopes of the retarding potential curves giving the energy distribution functions. Data are given for atomically clean Mo and for Mo covered with a monolayer of gas. Corresponding retarding potential and energy distribution curves for electrons ejected by 80-ev He^{++} ions are shown in Fig. 11.

The retarding potential curves are plots of the quantity $\rho=I_S/(I_T+I_S)$ *versus* V_r, the retarding potential between electrodes S and T corrected for the contact potential as determined by retardation of thermionic electrons emitted from the heated target (see Fig. 12). Satisfactory interpretation of the $\rho(V_r)$ curves demands consideration of the behavior with respect to V_r of the various space currents which may flow between electrodes S and T. These are the currents defined under the heading "Particle Currents" in Table I and depicted in Fig. 4.

We consider first singly charged ions ($z=1$). For V_r sufficiently negative (S positive re: T) the current I_i^e is collected at S *in toto*, but the currents I_i^i, I_{ie}^e, I_{ii}^e, and I_{im}^e are completely suppressed making $I_S=-I_i^e$ and $\rho=-\gamma_i=-I_i^e/I^i$. On the other hand, for V_r sufficiently positive, I_i^e is retarded out leaving only the secondary and tertiary currents which result from

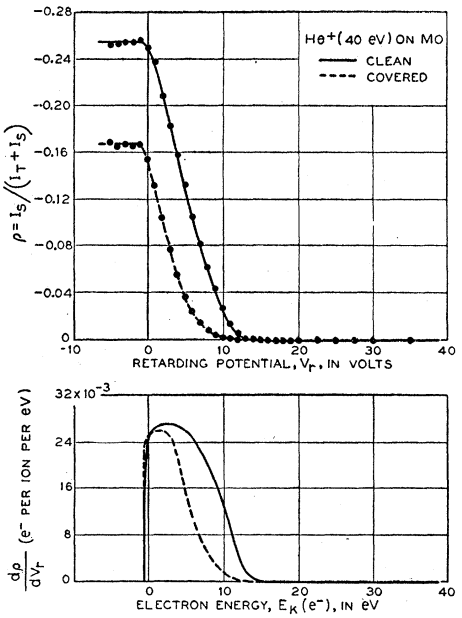

FIG. 8. Retarding potential curves (top) and electron energy distribution functions derived from them (bottom) for electrons ejected by 40-ev He^+ ions from clean Mo and from Mo covered with a layer of adsorbed gas.

reflection of primary ions as ions or metastable atoms. Thus, for singly charged ions $I_S=I_i{}^i+I_{ii}{}^e+I_{im}{}^e$ and $\rho=R=R_{ii}+\gamma_i'R_{ii}+\gamma_m'R_{im}$. These extreme values of ρ are indicated in Fig. 10 where R has the largest observed value.

Between the extremes of V_r discussed above, $\rho\cong-f_k\gamma_i+R$. The approximate equality in this expression is necessary because ρ is distorted by other effects such as the variability of δ' with V_r, the loss of electrons through the entrance aperture, and the distortion resulting from the failure of the target-collector geometry to meet the point-sphere ideal. The first two of these effects are small in this experiment, of the order of a few percent at most, and will not be discussed further here. The third effect represents a possibly more serious distortion of the energy distribution function. It is introduced by the fact that the target, though small relative to the collector sphere, is nevertheless plane. This tends to make electrons appear to

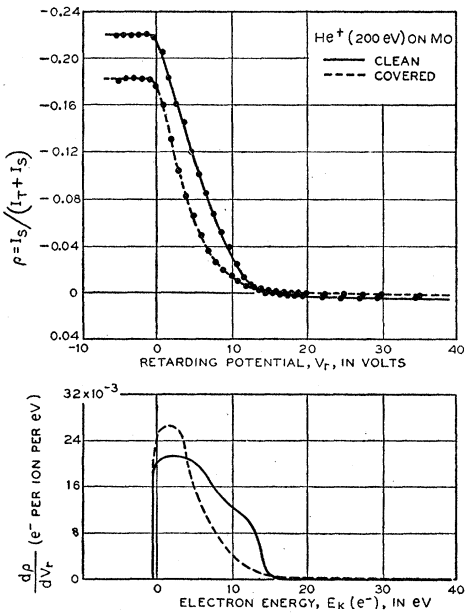

FIG. 9. Retarding potential curves (top) and energy distribution functions derived from them (bottom) for electrons from 200-ev He^+ ions on clean and covered Mo.

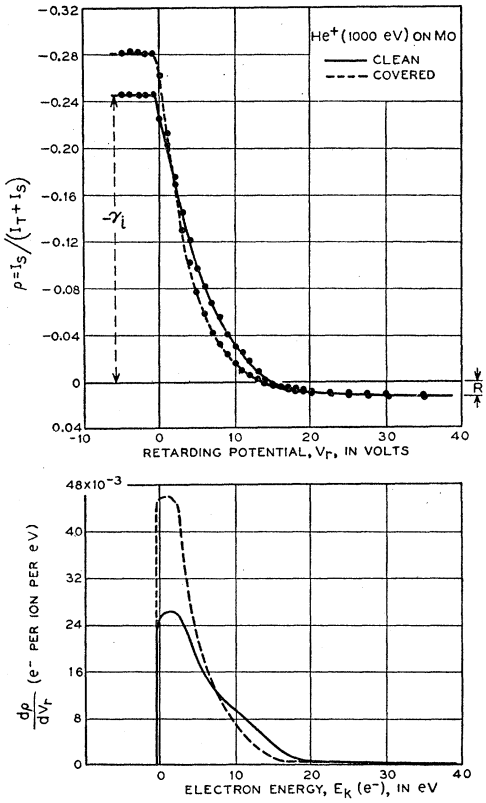

FIG. 10. Retarding potential curves (top) and energy distribution functions (bottom) for electrons from He^+ ions of 1000-ev energy at the target.

have smaller energies than they really do since the plane parallel retardation near the target operates only on the normal component of the electron's velocity. Electrons for which θ' (Fig. 7) is near 90° will be returned to the metal at much smaller V_r than $E_k(e^-)$. An energy distribution may thus appear to include electrons of zero energy even though, in fact, it does not. To the extent this limitation can be neglected the energy distribution function is $d\rho/dV_r=-\gamma_i(df_k/dV_r)$ for $V_r>0$ since in this region R is constant.

ρ *versus* V_r does not saturate at $V_r=0$, resulting in $d\rho/dV_r$ having a value for a limited range with $V_r<0$, because of retardation of the secondary ionic and

tertiary electronic currents in this region and the acceleration to S of electrons lost through the entrance aperture when the field is zero or retarding (see Fig. 12). The rapid saturation of ρ with decreasing V_r, however, indicates that the tertiary electronic currents soon have difficulty in finding the small target against a retarding field and that the reflected ions are of low velocity. R is constant for $V_r>0$ because the secondary ionic and tertiary electronic currents are then accelerated from one electrode to the other.

For doubly charged ions $z=2$ and γ_i expressed in electrons per incident ion is equal to $z\rho=2\rho$ for V_r sufficiently negative. Secondary and tertiary currents can flow when the current I_i^e is suppressed in this case also. These currents result from reflection of the doubly charged ion as a doubly charged ion, a singly charged ion, or a neutral atom, the latter two possibly excited. They were found to be very small in this experiment (Fig. 11).

No significant change in the form of the kinetic energy distribution function for electrons from He^+ is seen to occur with increasing ion energy (Figs. 8, 9, and 10). This is to be expected from the theory of

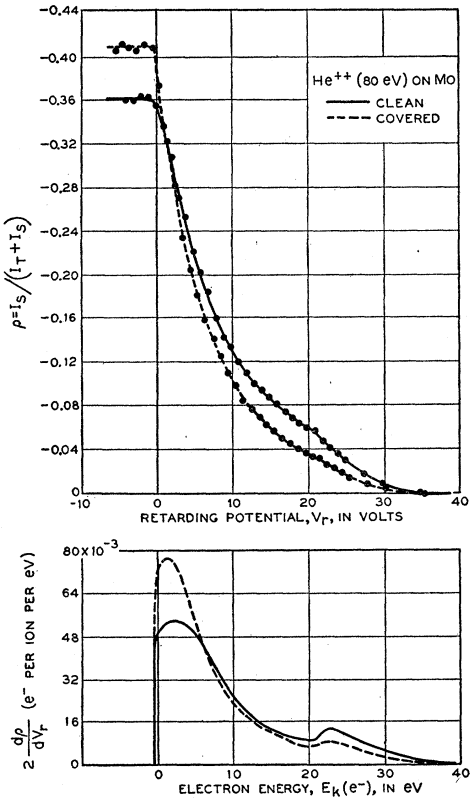

FIG. 11. Retarding potential curves (top) and electron energy distribution functions derived from them (bottom) for He^{++} ions of 80-ev energy incident upon clean Mo and upon Mo covered with a layer of adsorbed gas. Note that the energy distribution in number of electrons per incident ion per electron volt energy range is $2(d\rho/dV_r)$ for He^{++} since the ion is doubly charged ($z=2$).

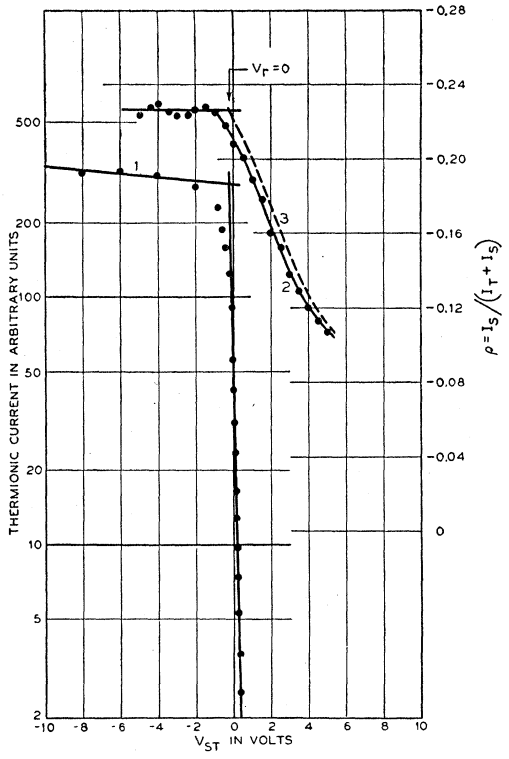

FIG. 12. Data for determination of contact potential between target and electron collector (electrodes T and S, respectively) in the experimental apparatus. Curve 1 shows the variation with V_{ST} of the current of thermionic electrons emitted from the heated target. The crossing of the extrapolated straight line portions of this curve determines the point of zero field at $V_{ST}=-0.2$ volt. Curve 2 is a part of the retarding potential curve for electrons from 200-ev He^+. Why it saturates at negative values of the corrected retarding potential $V_r(=V_{ST}+0.2$ ev in this case) is explained in Sec. VI of the text. Curve 3 is representative of the curve as it would appear if the effects of secondary and tertiary currents and electron loss through the entrance aperture in S could be corrected for.

potential ejection although kinetic ejection might conceivably result in a similar independence of distribution function and ion energy. The theory of potential ejection has not been developed to the point where a reliable distribution function can be derived. However, the two stage process of Fig. 1, which theory indicates is the predominant one, should yield the same electron energy distribution function for He^+ ions incident on a metal surface as is observed for the metastable atoms, He^M.[33] The distributions observed for He^+ are in approximate agreement with the distributions observed by Oliphant[14] and Greene[15] for electrons from He^M. In particular, in agreement with Greene, it seems difficult to account for the observed distribution for He^+ as being Maxwellian and resulting from thermal emission of the electrons.[34] There are serious discrepancies be-

[33] This conclusion is supported by the Townsend discharge measurements of J. P. Molnar, Phys. Rev. 83, 940 (1951), which show $\gamma_i(A^+)$ and $\gamma_m(A^M)$ on several targets to be closely equal.

[34] A theory of thermal emission of electrons from a spot on the target surface heated by dissipation of the ion's *kinetic* energy

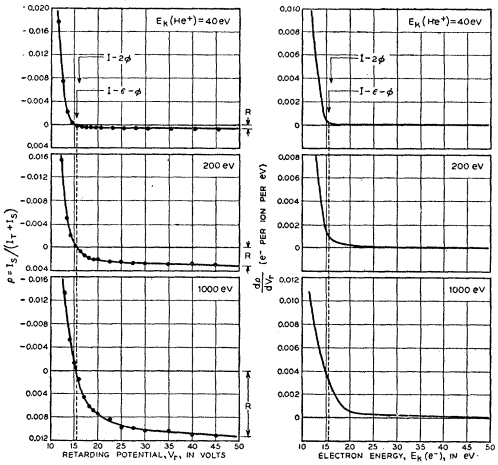

FIG. 13. Portions of the retarding potential curves of Figs. 8, 9, and 10 near the upper electron energy limit plotted (left) to an extended ordinate scale and the corresponding portions of the energy distribution functions (right). Energy limits predicted by the two potential ejection mechanisms discussed in the text in Sec. II are indicated above the top curves. Definition of the quantity R in terms of ejection and reflection coefficients is given in Table I. Note the agreement of the upper limit with theory at low $E_k(He^+)$, and the increase in R and the appearance of electrons of energies beyond the theoretical limits with increase in $E_k(He^+)$.

tween the distributions of electrons ejected by He^+ observed by Oliphant[11] and those observed in this work, however.

The effect of a layer of adsorbed gas atoms on the target surface is seen to reduce the number of fast electrons relative to the number of slow electrons. It appears to be true at ion energies for which γ_i increases or decreases from clean to covered target. The adsorbed layer does not appreciably shift the break in the retarding potential curves near $V_r=0$. A careful measurement shows the shift of the break and hence the variation of target work function to be no more than a few tenths of an electron volt.

In the distribution of electrons from He^{++} (Fig. 11), there is evidence of electrons having energies beyond 30 ev but none detectable which received all the energy available by neutralization of He^{++} directly to the ground state of He. On the other hand the mean energy of about 8 ev for electrons from He^{++} (compare the approximate 6-ev mean for electrons from He^+) would indicate sharing of the potential energy with several electrons as discussed in Sec. V. The structure observed in the distribution function of Fig. 11 remains unexplained.

VII. LIMITS OF KINETIC ENERGY OF EJECTED ELECTRONS

It is the purpose in this section finally to discuss the observed limits of ejected electron energy in the light of the predictions of theory.

All experimental observations of the lower energy limit show it to be zero. As has been pointed out this can result, in part at least, from the plane geometry of the target surface. Calculation of the apparent energy distribution function as would be measured in plane parallel geometry for the case represented in Fig. 7 indicates that this effect alone cannot account entirely for the experimentally observed form of the distribution function. It seems further necessary to assume that electrons suffer energy losses on leaving the metal, a conclusion perhaps not at variance with the observation that adsorbed gas on the surface decreases the relative number of fast electrons.

The present work agrees with Greene's observation[15] of electrons of zero energy released by He^M. Of Greene's four possible reasons for this observation, those attributing it to incorrect values of W_a or of contact potential can no longer be entertained. No serious error in the value of W_a given in Table II seems possible. Contact potential was measured in this experiment. The behavior of γ_i with $E_k(He^+)$ makes improbable the third reason attributing the electrons near zero to kinetic ejection. Energy loss at the metal surface remains the most probable explanation.

Oliphant's conclusion[14] that no electrons of energy less than 1.9 ev are ejected by He^M is most likely to be attributed to a failure of his method of determining the contact potential between target and electron collector. Oliphant's energy distributions for electrons from He^+ on Mo[11] show electrons of zero energy but possess other characteristics very difficult to explain. Evidence is presented by Oliphant of electrons in quantity having energies in excess of 20 ev. To account for these electrons, Oliphant and Moon[5] proposed the possibility of ions being neutralized inside the potential barrier of the metal where they could eject electrons of maximum energy $I-\phi=20.3$ ev. Theory of the predominant two stage process predicts a maximum energy of 15.5 ev (Table III). The present results do not support the view of Oliphant and Moon. It is perhaps possible to explain Oliphant's result if his ion beam (not m/e analyzed) contained an appreciable admixture of He^{++} ions.

In Fig. 13 retarding potential data in the vicinity of maximum electron energy are plotted to an extended ordinate scale. From these graphs three interesting conclusions may be drawn: (1) At low $E_k(He^+)$ a rather well defined upper limit of $E_k(e^-)$ is observed agreeing well with the predictions of theory. (2) As $E_k(He^+)$ is increased the quantity R ($=\rho$ at large positive V_r) is seen to increase indicating greater reflection of ions as ions and metastable atoms at higher

was proposed by P. L. Kapitza, Phil. Mag. **45**, 989 (1923) and discussed further by N. D. Morgulis, J. Exptl. Theor. Phys. (U.S.S.R.) **4**, 449 (1934); **9**, 1484 (1939); **11**, 300 (1941), and by S. V. Izmailov, J. Exptl. Theor. Phys. (U.S.S.R.) **9**, 1473 (1939). The theory does not account for the observed dependence of kinetic ejection on work function [H. Paetow and W. Walcher, Z. Physik **110**, 69 (1938)] nor the dependence on ion mass of kinetic ejection by isotopic ions [W. Ploch, reference 4].

ion energies. (3) Small numbers of electrons possessing energies in excess of the theoretical limits are produced as the incident ion energy is increased. This last conclusion is based on the assumption that R is independent of V_r in this region. This is eminently reasonable since the incident ion energy at the target surface is independent of V_r and all secondary and tertiary currents resulting from reflection of ions as ions or metastable atoms are then accelerated by V_r. Changes in slope of the $\rho(V_r)$ curve are thus attributed to retardation of the electron current (I_i^e) ejected by the primary ion current. It should be noted that the number of electrons observed beyond $V_r=15.5$ v is very small representing at most only about 1 percent of all electrons ejected by 1000-ev He^+.

In view of all other aspects of the phenomenon, the electron current observed at $V_r>15.5$ v is most probably the result of potential ejection occurring when the incoming atom is very close to the metal surface where the atomic energy levels are shifted by the proximity of the metal. The theories discussed in Sec. II all assume the energy levels of the atomic particle to be undisturbed on approach to the metal surface. Considerations of the potential energy of interaction of the particles He, He^M, and He^+ with the surface atoms of a metal show that the levels must shift and that electrons faster than the limits $I-\epsilon-\phi$ could be produced by final decay of the metastable atom very close to the metal surface. The effect would be expected to become more pronounced at higher ion energies because the probability of decay at greater distances from the metal is reduced in inverse proportion to the ion's velocity.

Another possible explanation of the electrons having $E_k(e^-)>I-\epsilon-\phi$ attributes them to kinetic ejection by the incident ions or by the normal atoms resulting from ion neutralization. The probability of ejection by this mechanism would also be expected to increase with increasing ion energy as is observed.

The maximum energy of electrons produced by ions incident on a gas covered surface appears, in Fig. 8 for example, to be less than that for a clean surface. This is not the case; the appearance of the curves of Fig. 8 results from the much smaller number of faster electrons produced at the gas covered surface. If the data are plotted to relative ordinate scales which make the slopes of the curves appear equal at $V_r=10$ v, breaks like those at the upper left of Fig. 13 appear in both curves at the same energy. This is in agreement with the observation recorded above that the adsorbed layer changes the work function of the target by at most a few tenths of an electron volt.

The author wishes to express his gratitude to his colleagues C. Herring, J. A. Hornbeck, J. P. Molnar, G. H. Wannier, and A. H. White for helpful discussions during the course of the work; to H. W. Weinhart under whose supervision the experimental tube was constructed; and to F. J. Koch for technical assistance.